Nanochem Res 5(2): 185-196, Summer and Autumn 2020

RESEARCH PAPER

Sensitive amperometric detection of hydrazine using a rutin/ graphene-chitosan nanocomposite modified glassy carbon electrode

Mahmoud Roushani[1,*], Kobra Bakyas[1], Behruz Zare Dizajdizi[1], Azadeh Azadbakht[2]

[1] Department of Chemistry, Faculty of Science, Ilam University, Ilam, Iran

[2] Department of Chemistry, Khorramabad Branch, Islamic Azad University, Khorramabad, Iran

ARTICLE INFO

Article History:
Received 28 May 2020
Accepted 04 September 2020
Published 15 October 2020

Keywords:
Electrocatalytic oxidation
Hydrazine
Graphene-Chitosan nanocomposite
Rutin

ABSTRACT

The present study describes a new approach for the investigation of electrocatalytic oxidation of hydrazine by using a glassy carbon electrode (GCE) modified by graphene chitosan nanocomposite (Gr-Cs) and Rutin (Ru). The heterogeneous electron transfer rate constant (ks) and the surface coverage of immobilized Ru on the Gr–Cs/GCE were obtained as 63 s−1 and 4.48×10−11 mole cm−2, respectively. The designed sensor showed excellent electrocatalytic activity toward oxidation of hydrazine. The catalytic rate constant (kcat) of the modified electrode toward N2H4 is 6.3 ×103 M-1s-1. Linear relationship between amperometric current response and hydrazine concentration was observed in the range of 0.3-1500 µM and the limit of detection was 90 nM (S/N=3). In addition, the modified electrode has an excellent anti-interference property in the presence of other potentially interfering species as well as a good operational stability. To evaluate the applicability of the proposed sensor, it was employed to determine hydrazine in a drinking water sample.

How to cite this article
Roushani M., Bakyas K., Zare Dizajdizi B., Azadbakht A. Sensitive amperometric detection of hydrazine using a rutin/ graphene-chitosan nanocomposite modified glassy carbon electrode. Nanochem Res, 2020; 5(2):185-196. DOI: 10.22036/ncr.2020.02.009

INTRODUCTION

Hydrazine is the simplest diamine, a highly reactive base, and a reducing agent. It is widely used in wide areas such as fuel cells [1], rocket propellants, insecticides and explosives [2]. However, despite its wide range of applications, pure hydrazine is highly toxic and harmful to human life. Due to the toxicological nature of hydrazine compounds, it is necessary to develop sensitive and selective analytical methods for its detection and determination. So far, several techniques including spectrophotometry, potentiometry, titrimetry and chemiluminescence have been reported for the determination of hydrazine [3–6]. Electrochemical techniques have many advantages, like cost-effectiveness, sensitivity, simple operation and the ease of miniaturization [7–9]. However, the direct electrooxidation of hydrazine on conventional bare electrodes suffers due to the slow electron transfer kinetics. Thus, enhancing the oxidation current response of hydrazine is of constant interest in the development of novel materials [10, 11].

Various materials have been used to enhance the catalytic properties of the electrode and to increase the sensitivity of the electrochemical sensors. Graphene (Gr), a two-dimensional sheet of sp^2-bonded carbon atoms arranged in a honeycomb lattice, has been widely applied in the preparation of electrochemical sensors and biosensors [12]. Gr, due to its excellent properties including high electrical conductivity, large specific surface area,

* Corresponding Author Email: *m.roushani@ilam.ac.ir; mahmoudroushani@yahoo.com*

high electrocatalytic activity and good mechanical strength, is able to improve the electrocatalytic performance of the modified electrode's surface [13]. However, the aggregation of Gr nanosheets limits their application. Chitosan (Cs) is a polysaccharide biopolymer which reveals excellent film-forming ability, high water permeability, good adhesion and susceptibility to chemical modifications due to the presence of reactive amino and hydroxyl functional groups. Dispersing graphene in polymer matrix such as Cs prevents their aggregation and augments the electrochemical properties [14].

Rutin (3′, 4′, 5, 7 - tetrahydroxyflavone 3β-D-rutinoside) is a derivative of catechol and a biologically important molecule whose chemical structure is demonstrated in Scheme 1S [15]. Catechol derivatives have been used as electron transfer mediators in electrochemical processes, since they have excellent redox reversibility, high electron transfer efficiency and low cost [9].

In this study, we fabricated a novel electrochemical sensor based on the immobilization of Ru on the GCE modified by Gr-Cs nanocomposite. The proposed sensor is used for the electrochemical determination of hydrazine using the amperometric method. It shows a lower background current, primarily due to full charging the electrochemical double-layer capacitance in a short time scale, because the potential of the working electrode is fixed during time. Modified electrode demonstrated a higher electrocatalytic activity toward oxidation of hydrazine in comparison to bare GCE.

EXPERIMENTAL

Material and reagents

All solutions were freshly prepared with double distilled water. Hydrazine (N_2H_4), Ru, Cs, Gr and all other reagents were of analytical grade and obtained from Merck (Darmstadt, Germany). Phosphate buffer solution (PBS 0.1 M) was prepared by mixing the stock solution of 0.1 M NaH_2PO_4 and 0.1 M Na_2HPO_4, and the pH was adjusted by NaOH or HCl. All electrochemical experiments were carried out at a room temperature.

Apparatus

Electrochemical experiments were performed with a μ-AUTOLAB electrochemical system type III and FRA2 board computer controlled Potentiostat/Galvanostat (Eco-Chemie, Switzerland) driven with NOVA software in conjunction with a conventional three-electrode system. A modified GCE as the working electrode, an Ag/AgCl (satd 3.0 M KCl) as the reference electrode and a platinum (Pt) wire as the counter electrode were used. Scanning electron microscopic (SEM) images of the modified surfaces were acquired using a Vega-Tesacn electron microscope.

Preparation of the Ru/Gr-Cs/GC modified electrode

Prior to modification, the bare GCE (2.0 mm in diameter) was carefully polished to a mirror like surface with 0.3 and 0.03 μm alumina slurries, followed by ultrasonication in anhydrous ethanol and double distilled deionized water for 3.0 min, respectively. To prepare graphene-chitosan suspension, a chitosan solution (0.3%) was obtained by dissolving almost 0.003 gr of chitosan in 1.0 ml acetic acid, and then 1.0 mg graphene dissolved in 1.0 ml DMF was added in to chitosan solution, followed by ultrasonication for 2.0 h to form a homogenous mixture of Gr–Cs. Then, 10.0 μl of the Gr-Cs solution was cast on the surface of bare GCE and dried at room temperature to form a Gr-Cs film. In order to remove the loosely attached Gr-Cs, the modified electrode was slowly rinsed with double distilled water [16]. For adsorption of Ru on the surface of Gr-Cs/GCE, the electrochemical activation of the Gr-Cs/GCE was performed by 20 continuous potential cycling in the rage of -0.2 to 1.8 V at the scan rate of 100.0 mV s^{-1} n 0.1 M PBS (pH 7.0). Then, 10.0 μL solution of Ru (0.001 M) was directly dropped onto the surface of Gr-Cs/GCE and dried at room temperature. Then, the electrode was placed in a 0.1 M PBS. Subsequently, the potential was scanned for 30 cycles at the scan rate of 100.0 mVs^{-1} in the range of 0.0 V to 0.8 V to obtain a stable redox response for the surface coated film. The results demonstrated that the current response of the redox couples decreases at first and then remains almost constant. The obtained electrode was denoted Ru/Gr-Cs/GCE.

RESULTS AND DISCUSSION

Characterization of the Ru/Gr-Cs/GCE

The surface morphologies of Gr-Cs/GC and Ru/Gr-Cs/GC electrodes were investigated by SEM. Fig. 1 reveals the SEM images of Gr-Cs/GCE (Fig. 1A) and Ru/Gr-Cs/GCE (Fig. 1B). As can be seen from Fig. 1B, when Ru deposited on the surface of the electrode, a new film formed on the surface of Gr-Cs/GC electrode.

Fig. 2 shows the cyclic voltammograms of

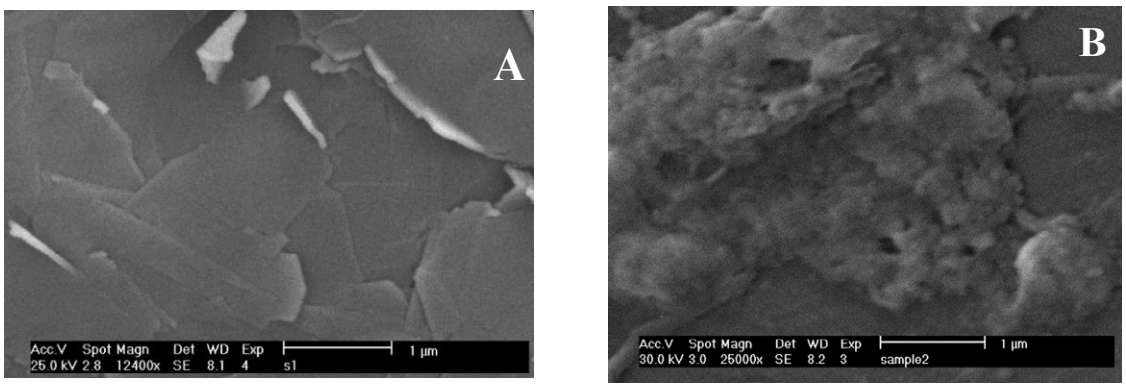

Fig. 1. SEM images of Gr-Cs/GC (A) and Ru/Gr-Cs/GC (B) electrodes.

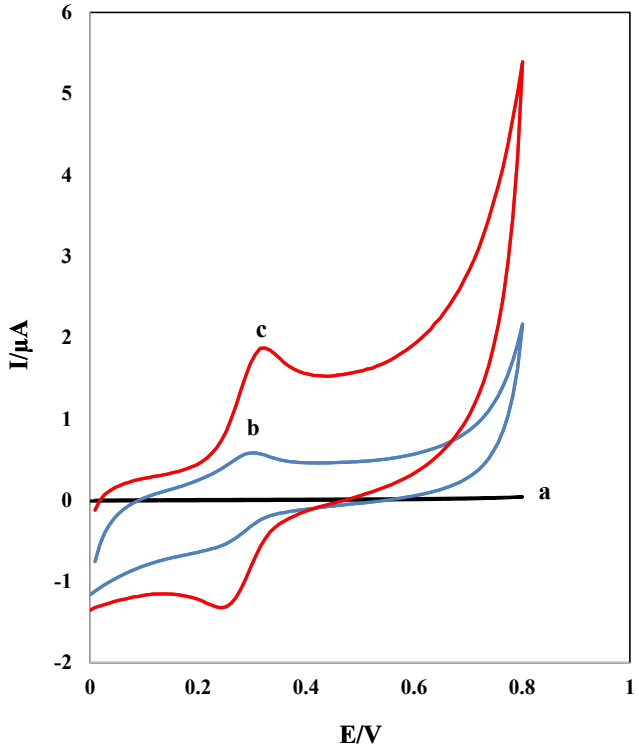

Fig. 2. CVs recorded in PBS (0.1 M, pH 7.0) for: (a) Gr-Cs/GC, (b) Ru/GC, and (c) Ru/Gr-Cs/GC electrodes, scan rate: 50 mVs^{-1}.

Gr-Cs/GC (a), Ru/GC (b) and Ru/Gr-Cs/GC (c) electrodes in phosphate buffer solution (pH 7.0). As can be seen, with Gr-Cs/GC electrode, at a potential range of the 0.0 to 0.8 V, no oxidation peak observed. A thin layer of Ru was formed on the surface of electrode by casting a drop of Ru solution (1.0 mM) on the bare GC and Gr-Cs/GC electrodes. In Fig. 2 (voltammogram c), for the Ru/Gr-Cs/GC electrode, a well-defined cyclic voltammogram with a peak potential separation of less than 50.0 mV and a peak current's height of 1.6 µA is observed. When we used bare GCE without Gr-Cs nanocomposite for adsorption of Ru, a cyclic voltammogram with very low current was obtained (voltammogram b). From these observations, it is concluded that high surface area of Gr-Cs nanocomposite leads to an excellent adsorption of Ru on the surface of electrode.

Effect of scan rate on the response of Ru/Gr-Cs/GCE

The effect of potential sweep rate was examined by the cyclic voltammetric response of R/Gr-Cs/GCE in a potential range of 0.0 to 0.8 V in PBS (0.1 M, pH 7.0). The sweep rate was varied in the range of 10–1000 mVs^{-1} (Fig. 3A). Both anodic and cathodic peak currents of Ru at Ru/Gr-Cs/GCE were increased with the scan rate (Fig. 3B). Moreover, the anodic peak currents were almost the same as the corresponding cathodic peak currents. The peak-to-peak potential separation was about 50.0 mV for sweep rates below 100.0 mVs^{-1} , suggesting facile charge transfer kinetics over this range of sweep rate.

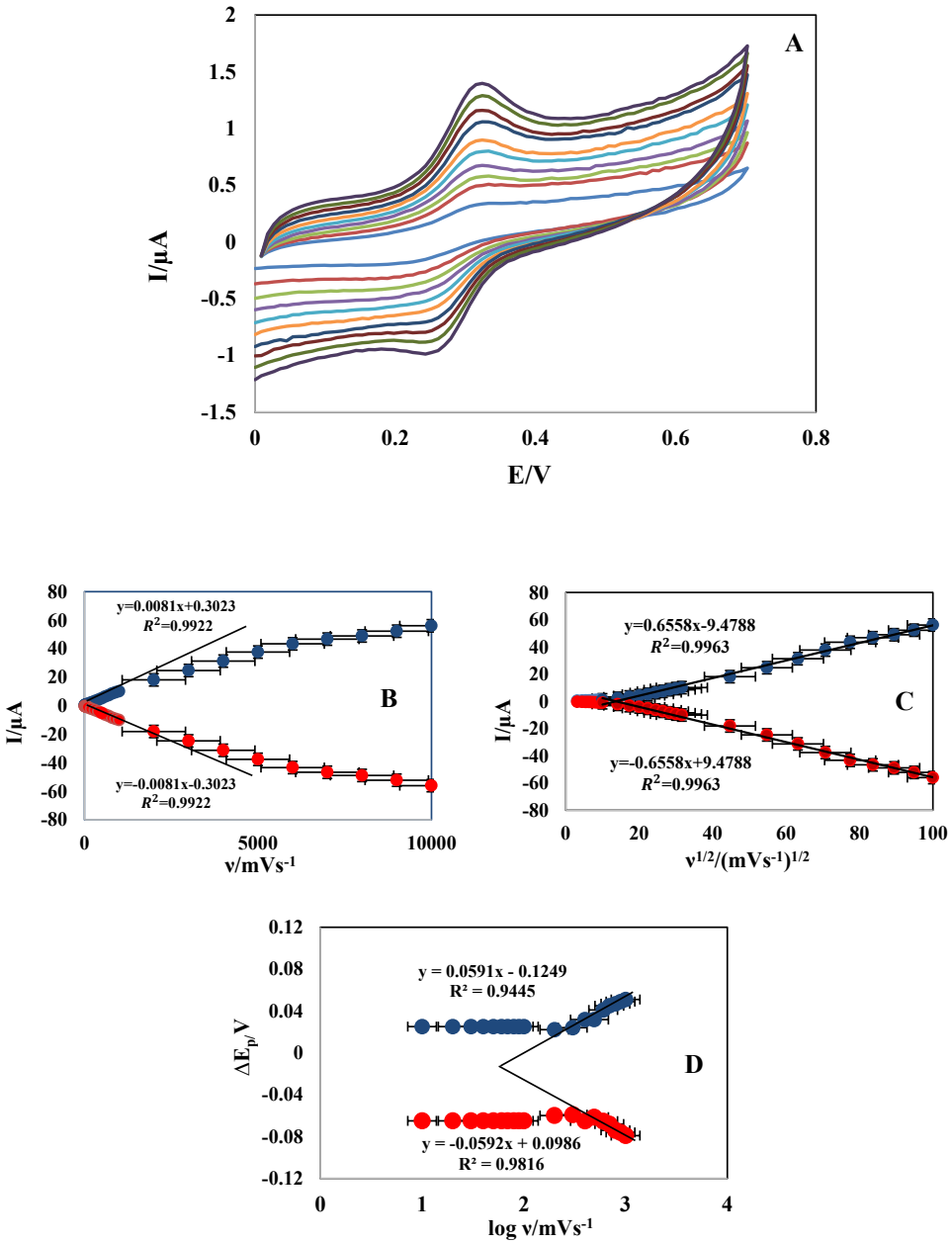

Fig. 3. A Cyclic voltammetric responses of a Ru/Gr-Cs/GCE in phosphate buffer (pH 7.0) at scan rates (inner to outer) of 10 –1000 mVs^{-1}. (B) And (C) plots of variation of the anodic and cathodic peak currents vs. the scan rate and square root of scan rate, respectively. (D) Variation of peak potential *vs.* logv.

Using the slope of I_p ersus v curve and according to the following equation, the surface concentration (Γ_c) of Ru on the surface of Ru/Gr-Cs/GCE was estimated [17],

$$I_p = \frac{n^2F^2vA\Gamma_c}{4RT} \quad (1)$$

where ν is the sweep rate, A is the geometric surface area of the electrode (0.07 cm^{-2}) and the other symbols have their usual meaning. Then, according to the slope of anodic peak currents versus scan rate, the calculated (Γ_c) of Ru is 4.48×10^{-11} cm^{-2}.

At higher sweep rates, the plots of peak currents vs. scan rate out of linearity and the peak current have a linear relationship to the square root of the scan rate (Fig. 3C), indicating a diffusion-controlled process. At sweep rates higher than 1000 mVs^{-1}, the peak potentials shifts and I_p ere proportional to the logarithm of the scan rate. Using the Laviron's theory [18], the electron transfer rate constant (k_s) and charge transfer coefficient (α) can be determined by measuring the variation of peak potential with scan rate. The peak potential values were proportional to the log (ν) for scan rates higher than 1500 mVs^{-1} (Fig. 3D). Also, the slope of the E_p versus log (ν), was about 59.1 mV. According to the equation $E_p = K - 2.3030(RT/\alpha nF)\log v$,and n=2 for Ru, a charge transfer coefficient of α=0.5 was obtained. By this α value and using the following equation:

$$\log k_s = \alpha\log(1-\alpha) + (1-\alpha)\log\alpha - \log(RT/nFv) - \alpha(1-\alpha)(nF\Delta E/2.3RT) \quad (2)$$

the electron transfer rate constant, k_s= 63.0 S^{-1} was estimated.

According to the high value of the electron transfer rate constant, Gr-Cs composite has an excellent ability for promoting electrons between Ru and the electrode surface.

Cyclic voltammograms of the Ru/Gr-Cs/GC electrode in phosphate buffer solution (0.1 M) at different pH values from 1.0 to 8.0 were recorded in order to study the effect of pH on the redox response of the modified electrode. As indicated in Fig. 4A, anodic and cathodic peak potentials of the Ru/Gr-Cs/GC electrode were changed into less positive values with the increase of pH values. The negative shift in peak potentials with the increase of pH indicates the participation of protons in the electron transfer reaction of Ru. Using the slope of $E^{0'}$. pH (slope=54.0 mv) results, the electrooxidation of Ru (shown in Fig. 4B) obeys the Nernst equation for a two-electron and two proton transfer reaction.

Electrocatalytic oxidation of hydrazine at Ru/Gr-Cs/GC electrode

According to high electron transfer rate constant of Ru at the Gr-Cs/GC electrode, it can be used as a mediator to shuttle electrons between electrode and analyte molecules. In order to examine the electrocatalytic activity of the Ru/Gr-Cs/GC electrode towards the oxidation of hydrazine, cyclic voltammetry techniques are used. Fig. 5A, B and C demonstrate the cyclic voltammograms of Ru/GC, Gr-Cs/GC and Ru/Gr-Cs/GC electrodes, respectively, in buffer solution (pH 7.0) in the absence (voltammogram a) and the presence (voltammogram b) of hydrazine. The results indicated that a significant peak current of hydrazine oxidation was observed with Ru/Gr-Cs/GC electrode. While no oxidation peak was observed at the surface of other electrodes in the absence or the presence of N_2H_4 in the potential range of 0.0 to 0.8 V, these electrodes were inactive to the direct oxidation of hydrazine. The results show that Ru has a high catalytic ability for hydrazine oxidation, and Gr-Cs nanocomposite on the base of large specific surface area properties provides accessible sites for adsorption of Ru on the surface of the electrode. Therefore, immobilized Ru onto the Gr-Cs nanocomposite could perform as a mediator to shuttle electrons between hydrazine and working electrode.

The cyclic voltammograms of Ru/Gr-Cs/GC modified electrode was recorded in the presence of different concentrations of hydrazine (Fig. 6). As shown, an anodic oxidation peak corresponding to hydrazine oxidation was observed at 0.35 V which increases proportionally with the increase of hydrazine concentration. The plot of I_p against hydrazine concentration indicates a linear correlation in the range of 0.006–0.4 mM which can be fitted into the equation;

I_p (μA) = 0.0586[hydrazine] (mM) + 2.8962 (μA).

The effect of scan rate on the electrocatalytic oxidation of hydrazine at the Ru/Gr-Cs/GCE was investigated by CV (Fig. 7A). As demonstrated in inset, the anodic peak currents are linearly proportional to the square root of the scan rates,

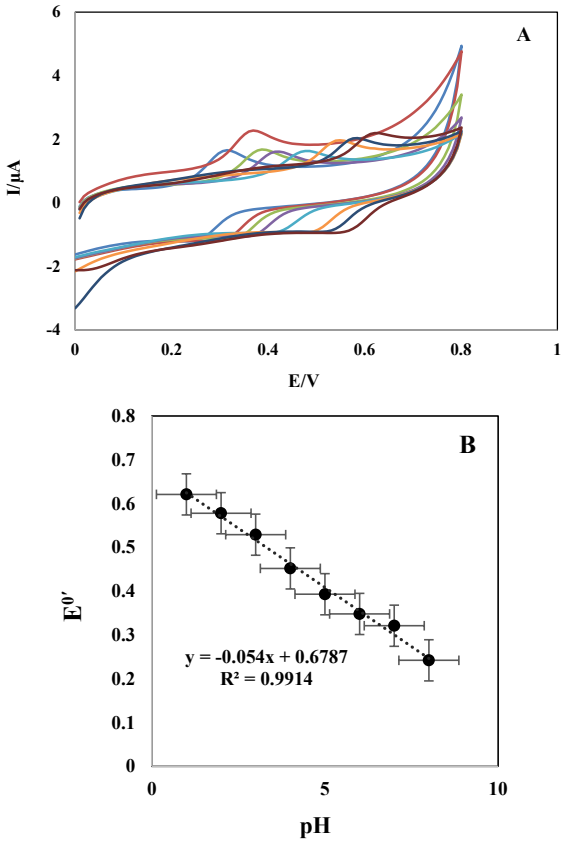

Fig. 4. A Cyclic voltammetric response of the Ru/Gr-Cs/GCE in different pH solutions of 2.0-8.0 (from right to left) at a scan rate of 50 mVs^{-1}. (B) The variation of formal potential *vs*. pH values.

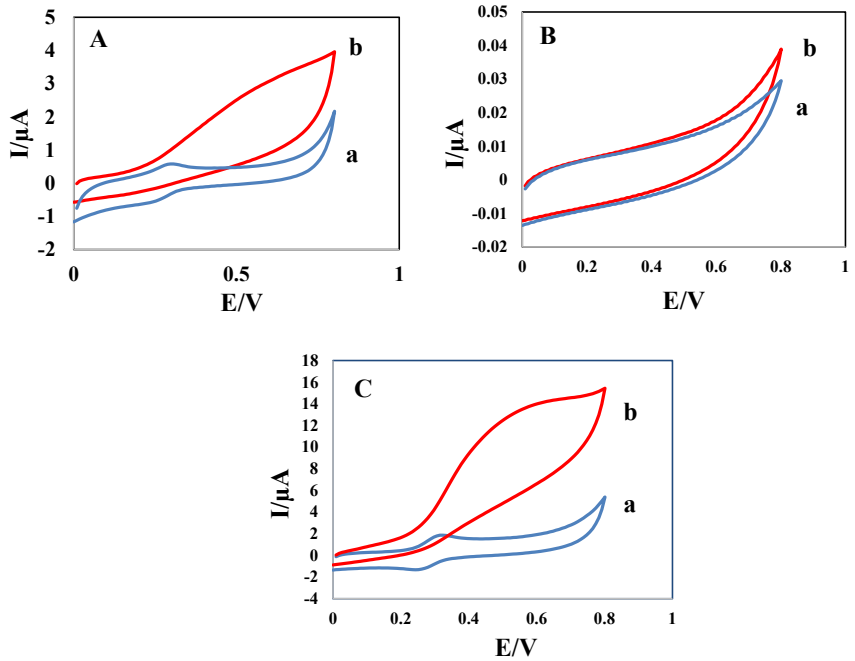

Fig. 5. CVs recorded in PBS (0.1 M, pH 7.0) in the absence (a) and presence (b) of 1.0 mM N_2H_4 for: (A) Ru/GC, (B) Gr-Cs/GC, and (C) Ru/Gr-Cs/GC electrodes, scan rate: 50 mVs^{-1}.

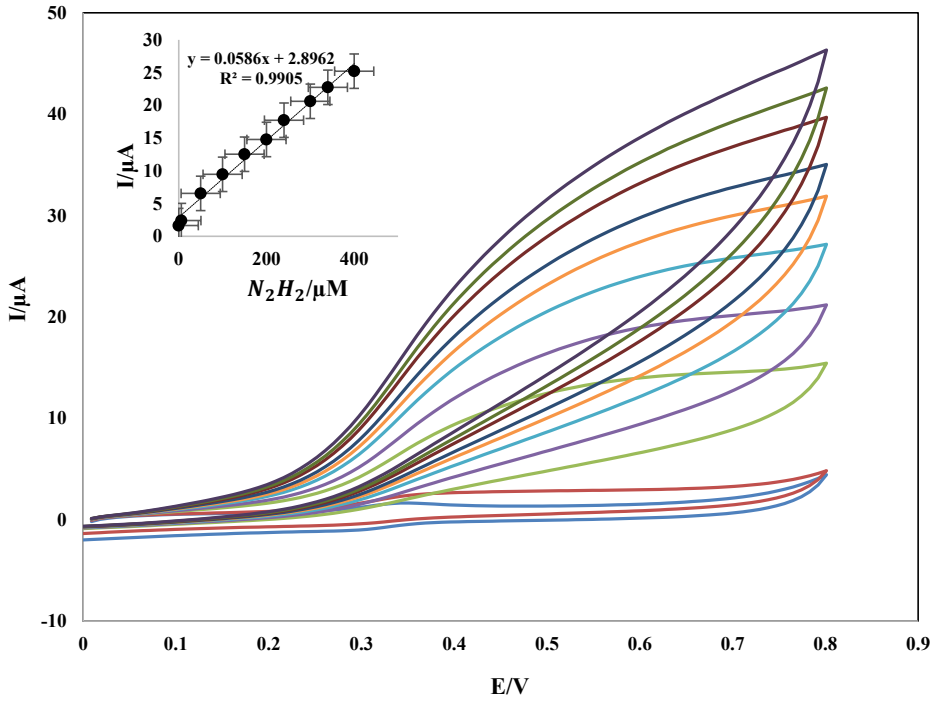

Fig. 6. Cyclic voltamograms of Ru/Gr-Cs/GCE in the presence of different concentrations of N_2H_4 in buffer solution (pH 7.0) from inner to outer 0, 0.006, 0.05, 0.1, 0.15, 0.2, 0.24, 0.3, 0.34 and 0.4 mM at scan rate 50 mVs^{-1}. The inset shows the catalytic response *vs.* N_2H_4 concentrations.

suggesting that the electrocatalytic oxidation of hydrazine on Ru/Gr-Cs/GC modified electrode is a diffusion-controlled process. Also, plots of the scan rate of the normalized current ($Ip/v^{1/2}$) vs. scan rate exhibited the characteristic shape of a typical EC′ catalytic process (Fig. 7B).

The mechanism for hydrazine oxidation at the Ru/Gr-Cs/GC electrode was proposed as follows:

Rutin (reduced form) → Rutin (oxidation form) + $2H^+ + 2\ e$ (3)

2Rutin (oxidation form) + N_2H_4 → N_2 +2 Rutin (reduced form) (4)

For *EC′* mechanism, Andrieux-Saveant theoretical model can be used to calculate the catalytic rate [24]. Based on this model, for a slow scan rate and a large catalytic rate, the relationship between the peak current and the analyte concentration is:

$$I_p = \alpha n F A D^{1/2} \left(\frac{Fv}{RT}\right)^{1/2} C_s \quad (5)$$

where D and C_s are the diffusion coefficient ($cm^2\ s^{-1}$) and the bulk concentration (mol cm^{-3}) of substrate (N_2H_4), respectively, and other symbols have their usual meanings. For low scan rates (10–20 mV s^{-1}), the average coefficient value (α) in Eq. (5) is found to be 0.32 for a Ru/Gr-Cs/GCE, with a surface coverage of 4.4×10^{-11} mol cm^{-2} and a geometric area A of 0.07 cm^2 in 0.05 mM N_2H_4 at pH 7.0. According to the approach of Andriex-Saveant, and using Fig. 1 in Ref. [24], the average value of the calculated k_{cat} is $6.3\times10^3\ M^{-1}\ s^{-1}$ for modified electrode. The high k_{cat} obtained for Ru/Gr-Cs/GCE implies that this system can be efficiently used as an electrochemical sensor for N_2H_4 detection.

Amperometric determination of hydrazine at Ru/Gr-Cs/GCE

Since fixed-potential amperometry is a simpler and usually more sensitive method than cyclic voltammetry, it was used to appraise the lower limit of detection for the proposed sensor. The amperometric response of the rotated Ru/Gr-Cs/GCE (rotation speed 1000 rpm) to the successive

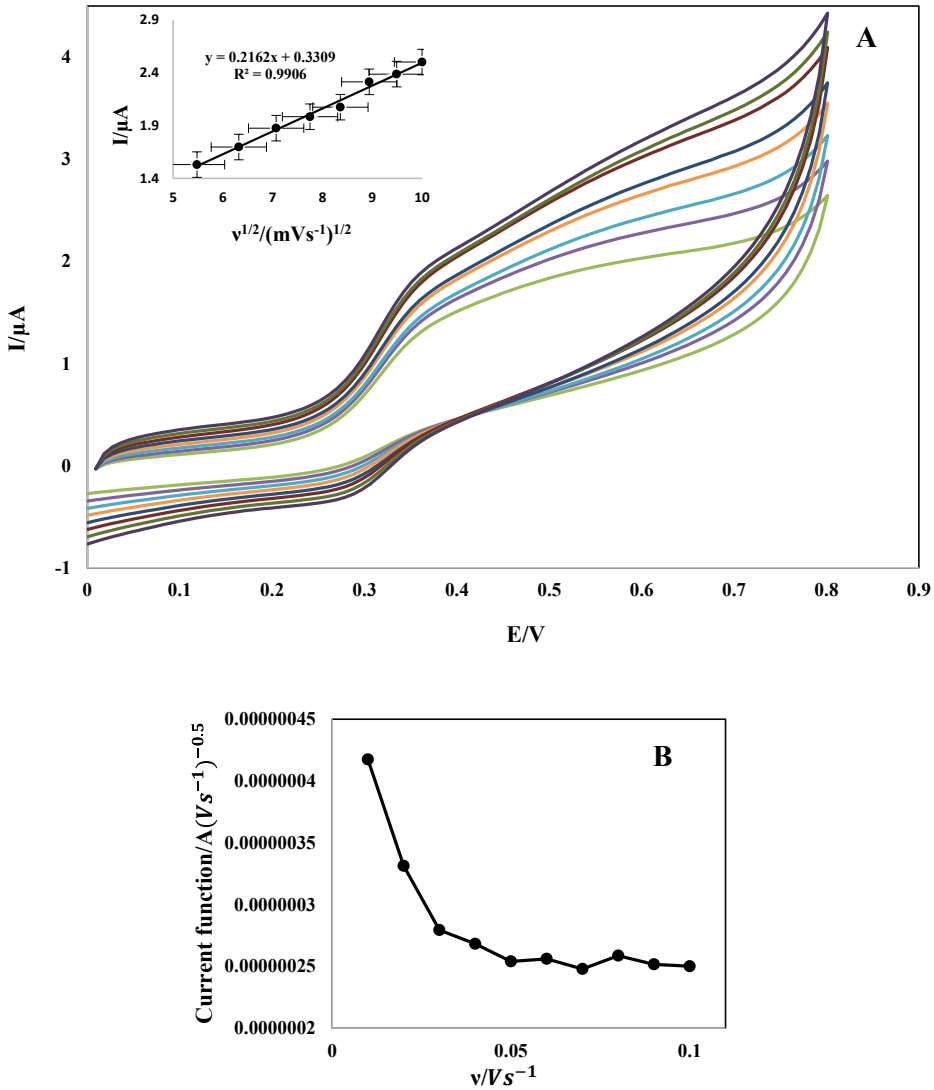

Fig. 7. A Cyclic voltammograms of Ru/Gr-Cs/GCE in the presence of 0.5 mM N_2H_4 in 0.1 M phosphate buffer solution (pH 7.0) at different scan rates (10–80 mVs^{-1}). Inset) Variation of peak currents with square root of potential scan rate. (B) Variation of normalized peak currents with potential scan rate.

injection of 0.3 µM, 1.0 µM and 0.1 mM of hydrazine in 10.0 ml 0.1 M PBS solution at 0.35 V (vs. Ag/AgCl) are demonstrated in Figs. 8A, B, and C, respectively. As can be seen, the modified electrode responded rapidly and approached 95% of the steady-state current within 3s. The plots of currents vs. hydrazine concentration are shown in insets of Fig. 8. Three linear ranges of 0.30–7.0, 1.0–18.0 and 200.0–1800.0 µM were obtained for hydrazine determination. The linear least squares calibration equation over the range of 0.30–7.0 µM was I/µA = 0.0536 [N_2H_4]/µM + 0.0173, with a correlation coefficient of 0.9957. The detection limit (signal to noise ratio of 3) was calculated as 90.0 nM, and the sensitivity of the sensor was 53.6 nA/µM. For a high concentration of hydrazine due to partial coverage of the electrode surface by adsorbed hydrazine and its oxidation products, the plot of current vs. N_2H_4 concentration deviates from linearity (inset of Fig. 8C).

The analytical performances of the constructed electrode and other electrodes for the detection of hydrazine are compared and listed in Table 1. based on the results, the analytical performances for Ru/Gr-Cs/GCE are comparable and even better than those obtained at several electrodes reported recently.

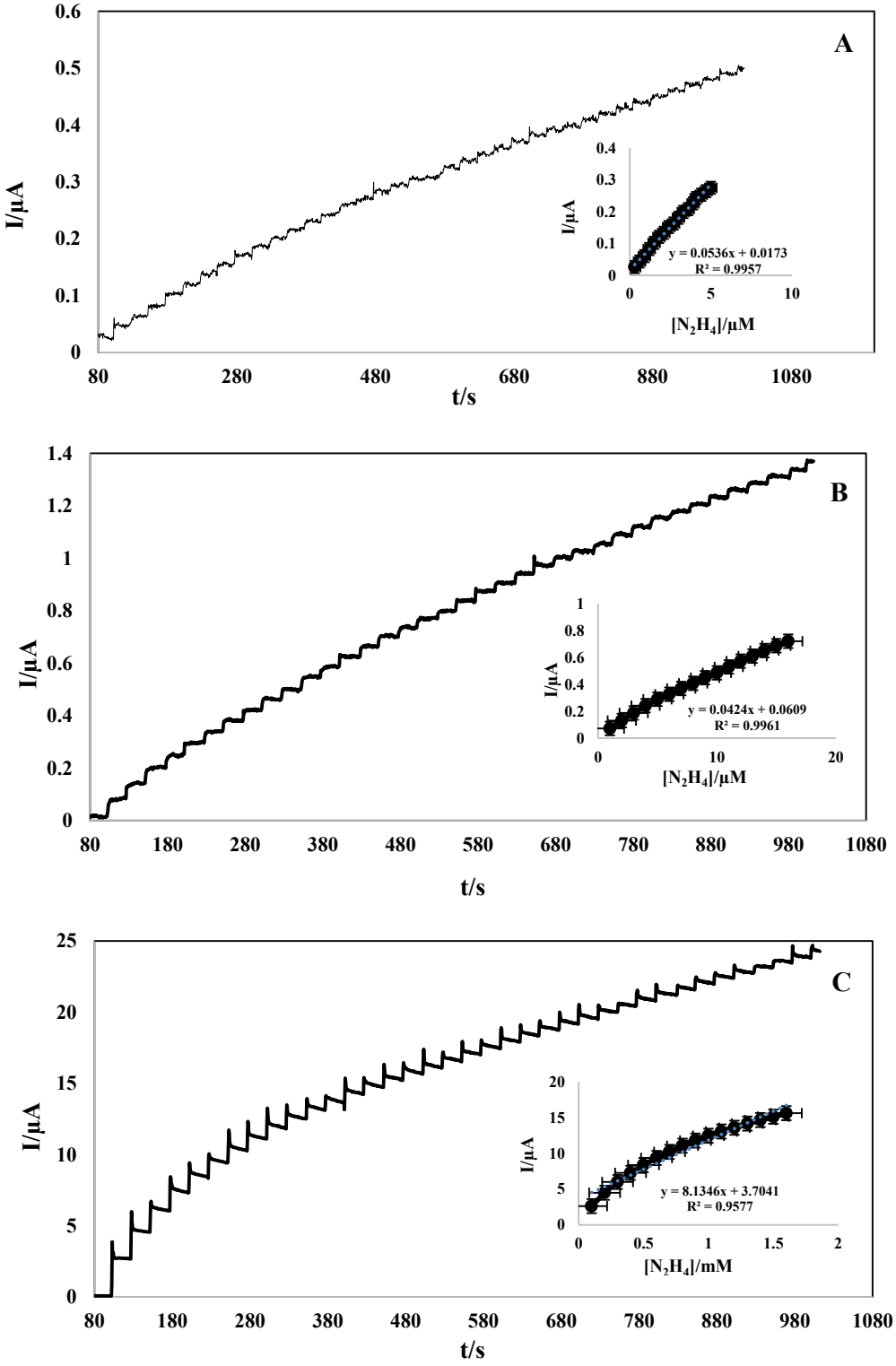

Fig. 8. Amperometric response for a rotating modified Ru/Gr-Cs/GCE at rotation speed 1000 rpm and 0.35 V in a pH 7.0 solution for successive additions of (A) 0.3 µM, (B) 1.0 µM and (C) 0.1 mM N_2H_4. The insets show plots of amperometric current vs. N_2H_4 concentrations.

Table 1. Comparison of the performances of various hydrazine sensors.

Electrode	Detection limit (μM)	Linear range (μM)	Applied potential (V)	Ref.
(Ni(II)–BA–MWCNT-PE)[a]	0.8	2.5–200	0.37	[8]
AuNP-GPE	3.07	0.05–250	0.30	[19]
HMWCNT[b] modified GCE	0.68	2–123	0.22	[20]
MnHCF[c] modified graphite–wax composite electrode	6.65	33.3–8180	0.45	[21]
PCV[d] modified GCE	4.2	5–500	0.3	[22]
o-AP[e] modified GCE	0.05	2–20	0.15	[23]
Ru/Gr-Cs/GCE	0.09	0.3–1500	0.35	This work

[a] Ni(II)–BA–MWCNT-PE: Ni(II)–baicalein multi-wall carbon nanotube paste electrode.
[b] HMWCNT: hematoxylin multi-wall carbon nanotubes.
[c] MnHCF: manganese hexacyanoferrate.
[d] PCV: pyrocatechol violet.
[e] AP: aminophenol.

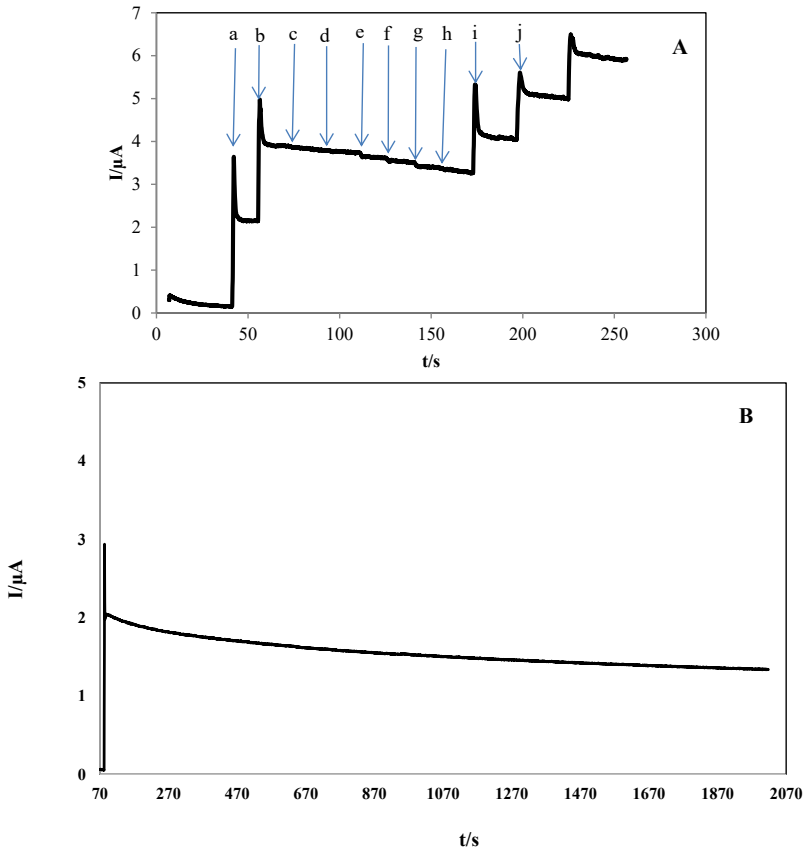

Fig. 9. A Amperometric response at Ru/Gr-Cs/GC electrode (rotation speed 1000 rpm) for the successive additions of 50 μM N_2H_4 (a and b), 5 mM sucrose (c), the same amount of glucose (d), $NaNO_2$ (e), Mg^{2+} (f), 2.5 mM Ca^{2+} (g), 2 mM Cd^{2+} (h), and 50 μM N_2H_4 (i and j) solutions in to the PBS. (B) Amperometric response of Ru/Gr-Cs/GC electrode (rotation speed 1000 rpm) held at −0.35 V in PBS (pH 7.0), for 25 μM N_2H_4 during 2000 s.

We also investigated the selectivity of the sensor towards common interfering species. Fig. 9A shows the amperometric response of Ru/Gr-Cs/GC modified electrode for successive addition of 50.0 μM hydrazine (a and b), 100 folds sucrose(c), glucose(d), $NaNO_2$(e), Mg^{2+}(f), 50 folds Ca^{2+}(g), Cd^{2+}(h) and 50.0 μM hydrazine (i and j) in a 10.0 mL 0.1 M PBS solution at 0.35 V. The increased initial current response was due to the addition of 50.0 μM hydrazine. After six additions, no changes of the current response were observed. Subsequently, 50.0 μM of hydrazine was added to the same solution and an increase of the current response was observed. The above experimental results indicate that the Ru/Gr-Cs/GCE has a good selectivity to hydrazine determination.

Another advantage of our proposed sensor was the highly stable amperometric response of the modified electrode toward hydrazine detection. The amperometric responses of Ru/Gr-Cs/GC modified electrode for 25.0 μM hydrazine were recorded over a continuous period of 2000 s (Fig. 9B). As shown, the response remained stable throughout the experiment, indicating that the Ru/Gr-Cs/GCE imparted higher stability for amperometric measurements of hydrazine.

To evaluate the applicability of the proposed sensor, it was employed to determine hydrazine in a drinking water sample. We measured the concentration of hydrazine in an artificially prepared specimen, by adding known amounts of N_2H_4 to water samples. The standard addition method was used for determination of N_2H_4 in this specimen. The recorded amperograms of the modified electrode and the calibration curve for sample 1 from Table 2 is shown in Fig. 10. The recovery percentage obtained by the method reveals the capability of the sensor for determination of hydrazine in drinking and river water samples. The results are shown in Table 2.

Table 2. Determination of hydrazine in water samples (n=3).

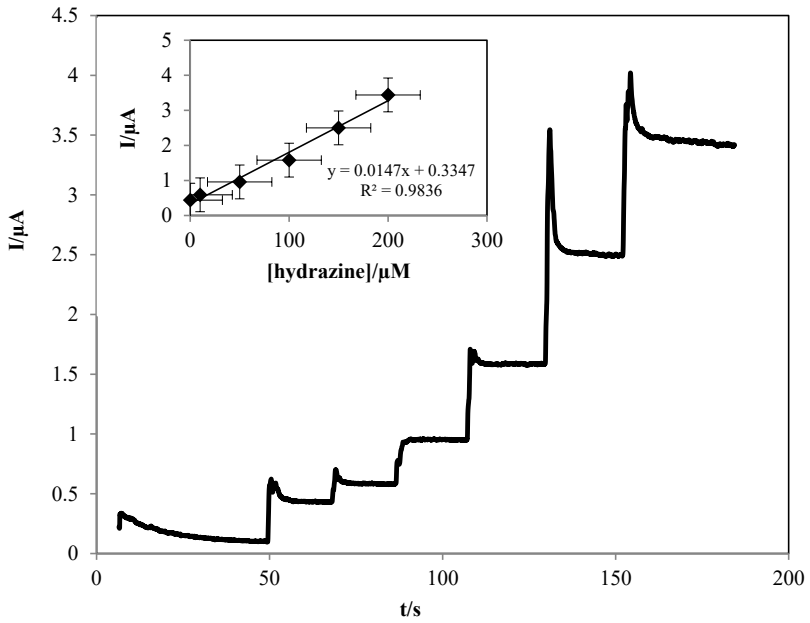

Fig. 10. Amperometric response of Ru/Gr-Cs/GC electrode (rotation speed 1000 rpm) held at 0.35 V in PBS (pH 7.0), and in real sample pH 7.0 (sample 1 from table 2) in the presence of different concentrations of N_2H_4 (0, 10, 50, 100, 150 and 200 μM). Inset) Plot of current vs. hydrazine concentration.

CONCLUSION

In this work, a novel sensor based on Ru/Gr-Cs nanocomposite was fabricated for the determination of N_2H_4, which exhibited significantly good electrochemical characteristics, including broad linearity (0.3 to 1.5 mM), excellent detection limit (90.0 nM), long-term stability and good sensitivity (53.6 nA/μM). The designed sensor showed excellent electrocatalytic activity with catalytic rate constant (k_{cat}) of 6.3×10^3 $M^{-1}s^{-1}$ toward oxidation of hydrazine. The special performance of this sensor can be attributed to the large surface area, excellent catalytic activity and high conductivity of graphene, the good biocompatibility and film-forming ability of chitosan, and the excellent catalytic activity of Ru.

CONFLICT OF INTEREST

The authors confirm that this article content has no conflict of interest.

REFERENCES

1. Yamada K, Yasuda K, Fujiwara N, Siroma Z, Tanaka H, Miyazaki Y, et al. Potential application of anion-exchange membrane for hydrazine fuel cell electrolyte. Electrochemistry Communications. 2003;5(10):892-6.
2. Ensafi AA, Mirmomtaz E. Electrocatalytic oxidation of hydrazine with pyrogallol red as a mediator on glassy carbon electrode. Journal of Electroanalytical Chemistry. 2005;583(2):176-83.
3. Safavi A, Ensafi AA. Kinetic spectrophotometric determination of hydrazine. Analytica Chimica Acta. 1995;300(1-3):307-11.
4. McBride W, Henry R, Skolnik S. Potentiometric Analytical Methods for Hydrazino Compounds. Sydrazine Sulfate. Analytical Chemistry. 1951;23(6):890-3.
5. Gawargious Y. Iodometric microdetermination of hydrazines by amplification reactions. Talanta. 1975;22(9):757-60.
6. Safavi A, Baezzat MR. Flow injection chemiluminescence determination of hydrazine. Analytica Chimica Acta. 1998;358(2):121-5.
7. Zhang H, Huang J, Hou H, You T. Electrochemical Detection of Hydrazine Based on Electrospun Palladium Nanoparticle/Carbon Nanofibers. Electroanalysis. 2009;21(16):1869-74.
8. Zheng L, Song J-f. Ni(II)–baicalein complex modified multi-wall carbon nanotube paste electrode toward electrocatalytic oxidation of hydrazine. Talanta. 2009;79(2):319-26.
9. Salimi A, Miranzadeh L, Hallaj R. Amperometric and voltammetric detection of hydrazine using glassy carbon electrodes modified with carbon nanotubes and catechol derivatives. Talanta. 2007.
10. Maringa A, Nyokong T. Behavior of Palladium Nanoparticles in the Absence or Presence of Cobalt Tetraaminophthalocyanine for the Electrooxidation of Hydrazine. Electroanalysis. 2014;26(5):1068-77.
11. Azad UP, Ganesan V. Determination of hydrazine by polyNi(II) complex modified electrodes with a wide linear calibration range. Electrochimica Acta. 2011;56(16):5766-70.
12. Rao CNR, Sood AK, Subrahmanyam KS, Govindaraj A. Graphene: The New Two-Dimensional Nanomaterial. Angewandte Chemie International Edition. 2009;48(42):7752-77.
13. Pang S, Tsao HN, Feng X, Müllen K. Patterned Graphene Electrodes from Solution-Processed Graphite Oxide Films for Organic Field-Effect Transistors. Advanced Materials. 2009;21(34):3488-91.
14. Schniepp HC, Li J-L, McAllister MJ, Sai H, Herrera-Alonso M, Adamson DH, et al. Functionalized Single Graphene Sheets Derived from Splitting Graphite Oxide. The Journal of Physical Chemistry B. 2006;110(17):8535-9.
15. Zare H, Samimi R, Nasirizadeh N, Mazloum-Ardakani M. Preparation and electrochemical application of rutin biosensor for differential pulse voltammetric determination of NADH in the presence of acetaminophen. Journal of the Serbian Chemical Society. 2010;75(10):1421-34.
16. Zheng M, Gao F, Wang Q, Cai X, Jiang S, Huang L, et al. Electrocatalytical oxidation and sensitive determination of acetaminophen on glassy carbon electrode modified with graphene–chitosan composite. Materials Science and Engineering: C. 2013;33(3):1514-20.
17. Brown AP, Anson FC. Cyclic and differential pulse voltammetric behavior of reactants confined to the electrode surface. Analytical Chemistry. 1977;49(11):1589-95.
18. Laviron E. General expression of the linear potential sweep voltammogram in the case of diffusionless electrochemical systems. Journal of Electroanalytical Chemistry and Interfacial Electrochemistry. 1979;101(1):19-28.
19. Abdul Aziz M, Kawde A-N. Gold nanoparticle-modified graphite pencil electrode for the high-sensitivity detection of hydrazine. Talanta. 2013;115:214-21.
20. Zare HR, Nasirizadeh N. Hematoxylin multi-wall carbon nanotubes modified glassy carbon electrode for electrocatalytic oxidation of hydrazine. Electrochimica Acta. 2007;52(12):4153-60.
21. Jayasri D, Narayanan SS. Amperometric determination of hydrazine at manganese hexacyanoferrate modified graphite–wax composite electrode. Journal of Hazardous Materials. 2007;144(1-2):348-54.
22. Golabi SM, Zare HR, Hamzehloo M. Electrocatalytic oxidation of hydrazine at a pyrocatechol violet (PCV) chemically modified electrode. Microchemical Journal. 2001;69(2):13-23.
23. Nassef HM, Radi A-E, O'Sullivan CK. Electrocatalytic oxidation of hydrazine at o-aminophenol grafted modified glassy carbon electrode: Reusable hydrazine amperometric sensor. Journal of Electroanalytical Chemistry. 2006;592(2):139-46.
24. Andrieux CP, Saveant JM. Heterogeneous (chemically modified electrodes, polymer electrodes) vs. homogeneous catalysis of electrochemical reactions. Journal of Electroanalytical Chemistry and Interfacial Electrochemistry. 1978;93(2):163-8.